A Comparison of Radiation Effects in Crystalline ABO4Type Phosphates and Silicates

3 authors, including:

Lynn Boatner
Retired - Oak Ridge National Laboratory
928 PUBLICATIONS   **22,833** CITATIONS

R. C. Ewing
Stanford University
958 PUBLICATIONS   **30,470** CITATIONS

Some of the authors of this publication are also working on these related projects:

Project   DOE NEUP (Nuclear Engineering University Program) under award DE-AC07-05ID14517 View project

Project   Nuclear Fuel Cycle View project

A comparison of radiation effects in crystalline ABO_4-type phosphates and silicates

A. Meldrum[1,*,†], L. A. Boatner[1] and R. C. Ewing[2]

[1] Solid State Division, Oak Ridge National Laboratory, Oak Ridge, TN 37831, USA
[2] The University of Michigan, Dept. of NE&RS, Ann Arbor, MI 49108, USA

ABSTRACT

The effects of ion irradiation in the ABO_4-type compounds were compared by performing experiments on four materials that include the most common crystal structures (monazite *vs.* zircon) and chemical compositions (phosphates *vs.* silicates) for these phases. Pure synthetic single crystals of $ZrSiO_4$, monoclinic $ThSiO_4$, $LaPO_4$ and $ScPO_4$ were irradiated using 800 keV Kr^+ ions. Radiation damage accumulation was monitored as a function of temperature *in situ* in a transmission electron microscope. The activation energies for recrystallization during irradiation were calculated to be 3.1–3.3 eV for the orthosilicates but only 1.0–1.5 eV for the isostructural orthophosphates. For the ion-beam-irradiated samples, the critical temperature, above which the recrystallization processes are faster than damage accumulation and amorphization cannot be induced, is >700°C for $ZrSiO_4$ but it is only 35°C for $LaPO_4$. At temperatures above 600°C, zircon decomposed during irradiation into its component oxides (i.e. crystalline ZrO_2 plus amorphous SiO_2). The data are evaluated with respect to the proposed use of the orthophosphates and orthosilicates as host materials for the stabilization and disposal of high-level nuclear waste. The results show that zircon with 10 wt.% Pu would have to be maintained at temperatures in excess of 300°C in order to prevent it from becoming completely amorphous. In contrast, a similar analysis for the orthophosphates implies that monazite-based waste forms would not become amorphous or undergo a phase decomposition.

KEYWORDS: zircon, monazite, metamictization, amorphization, radiation effects, plutonium, waste form.

Introduction

ZIRCON ($ZrSiO_4$) and monazite ($LnPO_4$: Ln = La, Ce, Nd) are members of the general ABO_4 mineral group (A = Ln, Ac, Sc, Y, or Zr, where Ln and Ac refer to the lanthanides and actinides, respectively, and B = Si or P). Both phases occur widely in nature and typically contain U or Th impurities substituting on the A-site. Hence, zircon is currently the most commonly used mineral for radiometric dating of the earth's crust. However, zircon is frequently found to be metamict (i.e. rendered amorphous by natural α-decay-event damage) despite containing <5000 ppm uranium, on average (Speer, 1982). Zircon is less often reported to contain microcrystalline ZrO_2 precipitates (e.g. Vance and Anderson, 1972). Monazite generally contains high concentrations of the light rare earth elements (*LREE*) and lower abundances of the heavy rare earth elements (*HREE*). Concentrations in excess of 25 wt.% $ThO_2 + UO_2$ have been reported in monazite (Grammacioli and Segalstad, 1978). Other naturally occurring ABO_4-type compounds include hafnon ($HfSiO_4$), thorite (tetragonal $ThSiO_4$), huttonite (monoclinic $ThSiO_4$), xenotime (YPO_4), and pretulite ($ScPO_4$).

Zircon and monazite have related crystal structures. The zircon structure is tetragonal ($I4_1/amd$, Z = 4) and consists of chains of alternating, edge-sharing AO_8 and SiO_4 coordina-

* E-mail: ameldrum@gpu.srv.ualberta.ca
† Present address: Department of Physics, The University of Alberta, Edmonton, Alberta, Canada T6G 2J1

tion polyhedra parallel to the *c* axis (Hazen and Finger, 1979). The zircon structure-type includes $ZrSiO_4$, $HfSiO_4$, tetragonal $ThSiO_4$, YPO_4, $ScPO_4$ and the suite of (*HREE*)PO_4 (Taylor and Ewing, 1978; Milligan *et al.*, 1982, 1983). A larger A-site cation (e.g. the *LREE*) distorts the crystal symmetry and introduces a ninth oxygen into the A-site coordination sphere, resulting in the monazite structure (Mullica *et al.*, 1984). The monazite structure is, in fact, a monoclinic ($P2_1/n$, Z = 4) derivative of the higher-symmetry zircon structure. Phases with the monazite structure include a monoclinic high-temperature polymorph of $ThSiO_4$ (huttonite) and the suite of (*LREE*)PO_4 (Taylor and Ewing, 1978; Mullica *et al.*, 1985). In the present work, we compare the effects of irradiation on $LaPO_4$ and monoclinic $ThSiO_4$ (monazite structure), as well as $ScPO_4$ and $ZrSiO_4$ (zircon structure). These four compounds span the range of chemistry (phosphates *vs.* silicates) and crystal structure (monazite *vs.* zircon) for these ABO_4-type compounds.

The effects of heavy-ion irradiation on zircon and monazite have important ramifications because of their proposed use as waste forms for the disposal of plutonium from dismantled nuclear weapons (Ewing *et al.*, 1995; Burakov *et al.*, 1996; Ewing *et al.*, 1996; Weber *et al.*, 1996) and mixed high-level nuclear waste (Boatner, 1978; Boatner *et al.*, 1980, 1981; McCarthy *et al.*, 1980; Boatner and Sales, 1988), respectively. The accumulated effects of irradiation could lead, for example, to a radiation-induced crystalline-to-amorphous transformation with a corresponding reduction in the chemical durability (i.e. increased leach rate: Ewing *et al.*, 1982; Tole, 1985) and to a relatively large volume increase of the waste form itself (e.g. Weber, 1990).

Experimental

Synthetic single crystals of $ZrSiO_4$ and $ThSiO_4$ were grown by a high-temperature solution process employing a lithium molybdate flux (Reynolds *et al.*, 1972). Single-crystal specimens of $ScPO_4$ and $LaPO_4$ were grown by employing a lead pyrophosphate flux (Boatner and Sales, 1988). TEM specimens were prepared by hand polishing and ion milling using 4 keV Ar^+ ions. The specimens were then irradiated *in situ* in the HVEM-Tandem Facility at Argonne National Laboratory using 800 keV Kr^+ ions with a flux of 1.7×10^{12} $cm^{-2}s^{-1}$. The specimen temperature was varied from -250 to $800°C$ by using a heating stage or a liquid-helium-cooled cooling stage. Electron diffraction was used to monitor the specimens as the irradiation progressed (Fig. 1). The critical amorphization fluence, defined as the minimum ion fluence for the disappearance of the electron diffraction maxima, was determined for all the compounds. The experimental error ($\sim20\%$) was determined by performing the irradiations three times at room temperature.

Results and discussion

Irradiation results

The amorphization fluence, in units of ions/cm^2, was converted to an equivalent displacement dose in units of displacements per atom (dpa) using TRIM-96 calculations (full cascades) to calculate the number of displacements per ion in the thickness of the sample (estimated at 100 nm: Wang, 1998; Meldrum *et al.*, 1999a). This conversion requires a knowledge of the atomic displacement energies (E_d) for the constituent atoms. For $ZrSiO_4$ and monoclinic $ThSiO_4$, we

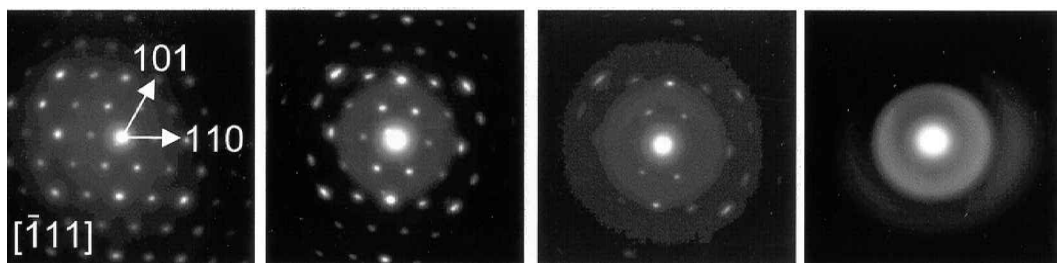

FIG. 1. Electron diffraction patterns observed during ion irradiation of $ZrSiO_4$. With increasing ion fluence, the initially sharp diffraction maxima gradually fade out and are replaced by an amorphous halo. The minimum ion fluence required for the complete disappearance of the electron diffraction maxima at each temperature was recorded and used to calculate the amorphization dose in Fig. 2.

used E_d values of 79 eV (A-site cation), 23 eV (Si), and 47 eV (O) (Weber *et al.*, 1998). The E_d values for the orthophosphates are not known, thus we used the same values as for the silicates.

The temperature dependence of the amorphization dose for LaPO$_4$, ScPO$_4$, monoclinic ThSiO$_4$, and ZrSiO$_4$ (e.g. one example each of the phosphates and silicates with either the monazite or zircon structure) is shown in Fig. 2. The measured amorphization dose reflects the competing effects of damage accumulation and recrystallization processes that occur during irradiation. In the case of the phosphates, the amorphization dose increases rapidly near room temperature. Above 60°C (LaPO$_4$: monazite structure) or 100°C (ScPO$_4$: zircon structure), amorphization can no longer be induced. On the other hand, the orthosilicates ZrSiO$_4$ and mono-clinic ThSiO$_4$ can be amorphized at temperatures as high as 700°C.

This large difference in the temperature dependence of the amorphization dose reflects a fundamental difference in the amorphization and recrystallization kinetics between the phosphates and silicates. This difference may be attributable to differences in the structure of the amorphous phases produced by irradiation. The PO$_4$ tetra-hedra are probably less readily polymerized than their silicate counterparts, owing to the presence of a double P−O bond. If the SiO$_4$ tetrahedra in amorphous silicates are indeed more highly polymerized, then a significant amount of bond breaking would be required to form a structure based on isolated SiO$_4$ tetrahedra (i.e. zircon). Additionally, the rigid PO$_4$ units may be more easily rotated or realigned during recrystallization.

For both the orthophosphates and orthosili-cates, the phases with the zircon structure (ScPO$_4$ and ZrSiO$_4$) can be amorphized at slightly higher temperatures than those with the monazite structure (LaPO$_4$ and monoclinic ThSiO$_4$). The monazite structure is thus more stable under irradiation at elevated temperatures; however, this difference is small compared to the chemical effect discussed above. At low temperatures, the measured difference for the monazite- and zircon-structure compounds was smaller and was close to experimental error, although the monazite struc-ture compounds still required a higher dose for amorphization. The effects produced by energetic ions may be slightly different in the monazite structure owing to a lack of ion channelling and linear collision sequences in the lower symmetry structure. This may lead to more compact collision cascades and less defect survival than would be expected to occur in the higher symmetry zircon structure (e.g. Robinson, 1983).
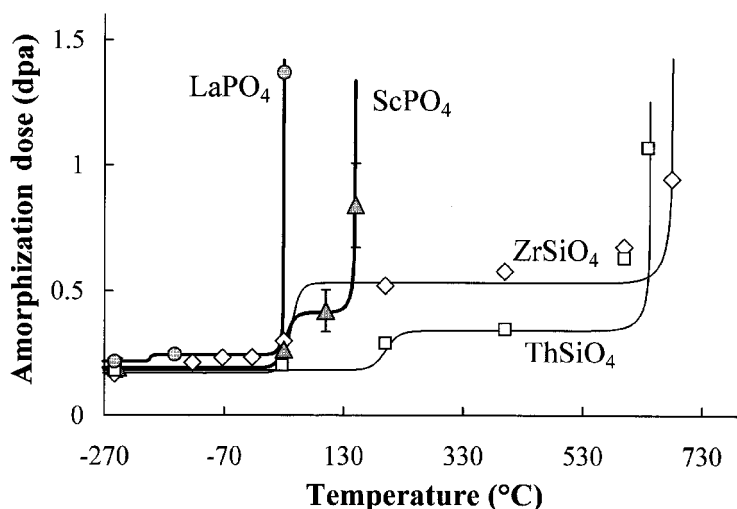

FIG. 2. Amorphization dose as a function of temperature for LaPO$_4$, ScPO$_4$, ZrSiO$_4$ and monoclinic ThSiO$_4$. The lines were calculated using equation 3. The jog in the calculated line for LaPO$_4$ at −200°C is not meant to imply the existence of a separate and defined recrystallization stage, but simply fits the model to the limited number of data points.

This difference may be sufficient to produce the small observed increase in T_c for the orthophosphates and orthosilicates with the zircon structure. Line crossing produced by the separate annealing stages (see below) complicates this analysis of intermediate temperatures.

For $ZrSiO_4$, $ThSiO_4$ and $ScPO_4$, the temperature dependence of the amorphization dose appears to increase in two separate stages (Fig. 2). Only a single stage was resolved in the case of $LaPO_4$. This two-stage behaviour appears to be outside of the experimental error. Similar behaviour was reported previously in the case of zircon irradiated with 1500 keV Kr^+ ions (Weber et al., 1994). The temperature dependence of the amorphization dose can be obtained by using one of several available models. The reader is referred to Weber et al. (2000) for a useful description of the difficulties and assumptions inherent in amorphization-recrystallization theories in general. According to a recently-developed model (Meldrum et al., 1999a), the amorphous volume fraction, f_a, increases with irradiation time, t, according to the following equation:

$$\frac{df_a}{dt} = P\left[1 - \varepsilon(1 - e^{-\lambda_I \cdot t})\right] \cdot (1 - f_a) - \lambda_{II} \cdot f_a \quad (1)$$

where P is the rate of production of amorphous zones ($P = 0.002$ dpa/s in the present experiments), ε is an empirical constant relating to the difference in the baseline amorphization dose for the two stages [$\varepsilon = (D_{0(II)} - D_{0(I)})/D_{0(II)}$, where $D_{0(I)}$ and $D_{0(II)}$ refer to the baseline amorphization dose (i.e. the flat part of the curves in Fig. 2)] for Stage I and Stage II, respectively. The terms λ_I and λ_{II} are the rate constants for recrystallization:

$$\lambda_n = A\exp(-E_{an}/kT) \quad (2)$$

where k = Boltzmann's constant and A is the lattice vibration frequency ($\sim 10^{13}$ Hz). The solution for equation 1, using the initial condition that $f_a = 0$ at $t = 0$, is given by:

$$f_a = \frac{P}{P + \lambda'} \cdot \left[1 - e^{-(P+\lambda')\cdot\left[(1-\varepsilon)\cdot t + \frac{\varepsilon}{\lambda_{cp}}(1-e^{-\lambda_{cp}\cdot t})\right]}\right] \quad (3)$$

where $\lambda' = \lambda/(1-\varepsilon)$ (Meldrum et al., 1999a). An amorphous volume fraction of 0.95 (Miller and Ewing, 1992) was assumed for the purpose of these calculations. Thus, the amorphous fraction at a given temperature is related to the activation energies for Stage I (E_{aI}) and Stage II (E_{aII}) recrystallization. E_{aI}, E_{aII}, and ε (Table 1) were selected to provide the best least squares fit to the data in Fig. 2, subject to the constraint that the curves pass through the highest temperature data point.

An expression for T_c, the critical temperature above which amorphization will not occur, can be derived from equation 1 (Meldrum et al., 1999a):

$$T_c = \frac{E_a}{k \cdot ln\left[\frac{A \cdot f_a}{P(1-\varepsilon)\cdot(1-f_a)}\right]} \quad (4)$$

T_c is the temperature above which the annealing processes are faster than those of damage accumulation. The values obtained for T_c are related to the dose rate P. When P is large (i.e. in the ion-beam experiments), then T_c is high. For the lower dose rates in minerals, T_c for a given mineral is correspondingly lower. The T_c values corresponding to the ion beam experiments and to 5 wt.% of incorporated Pu are given in Table 1 for the materials investigated here.

The physical meaning of the activation energies obtained from equations 1–3 are difficult to ascertain directly. However, the magnitudes of E_{aI} and E_{aII} may be characteristic of certain types of processes. For example, in the orthosilicates E_{aI} varies from $\sim 1 - 1.2$ eV. These values can be compared to the known defect migration energies in other insulating ceramics, as summarized in Zinkle and Kinoshita (1997). In general, the present values are similar to the interstitial migration energies in Al_2O_3 and MgO, but are slightly lower than the activation energies for

TABLE 1. Values of the terms used in equations 1–5.

	Phosphates		Silicates	
	$LaPO_4$	$ScPO_4$	$ZrSiO_4$	$ThSiO_4$
E_{aI} (eV)	–	1.0	1.0	1.2
E_{aII} (eV)	1.0	1.5	3.3	3.1
ε	–	0.54	0.68	0.47
C	1.05	1.56	0.66	3.4
X	260	220	170	302
T_c^1(°C)	300	420	700	650
T_c^2(°C)	−80	0	360	320

[1] T_c values for the ion-irradiation experiments ($P = 0.002$ dpa/s)

[2] T_c values for ^{239}Pu-doped material ($P = 10^{-12}$ dpa/s)

vacancy migration (these vary from 1.8 to 2.5 eV). On the other hand, the values obtained for E_{aII} (3.1−3.3 eV for ThSiO$_4$ and ZrSiO$_4$) are quite high. These could be associated with complex defect migration or, more likely, radiation-enhanced recrystallization of amorphous zones. This latter hypothesis is supported to some degree by the value of 3.6 eV recently obtained for the recrystallization of fission tracks parallel to the c axis in zircon (Virk, 1995).

On the other hand, the activation energies for Stage II recrystallization in the orthophosphates are considerably lower (1.0 and 1.5 eV for LaPO$_4$ and ScPO$_4$, respectively). The lower activation energies in the phosphates show that these materials are considerably more susceptible to recrystallization than their silicate analogues. This could explain the observation that natural monazite is only rarely reported to be metamict. For both the phosphates and silicates, the critical temperature was lower (i.e. more rapid annealing occurs) for the monazite structure types.

In the case of zircon, ion irradiation carried out at temperatures above 600°C produced a new effect. Above these temperatures, the zircon decomposed into its component oxides: cubic or tetragonal ZrO$_2$ + amorphous SiO$_2$ as a result of irradiation, as determined by electron diffraction, high resolution TEM (Fig. 3), and nanobeam EDS analysis. At temperatures between 600 and 750°C, the specimens become amorphous before decomposing, but at higher temperatures, the irradiated zircon decomposes directly to the component oxides without an intermediate amorphous phase. The ion fluence for these decompositions decreased with increasing temperature. A similar effect was observed in the case of monoclinic ThSiO$_4$ irradiated above 700°C; however, huttonite (unlike zircon) recrystallizes epitaxially from the thicker portions of the TEM grid at these high temperatures and so only small amounts of ThO$_2$ could be produced. These results were not duplicated by thermal annealing in the absence of irradiation at the maximum obtainable temperature (800°C).
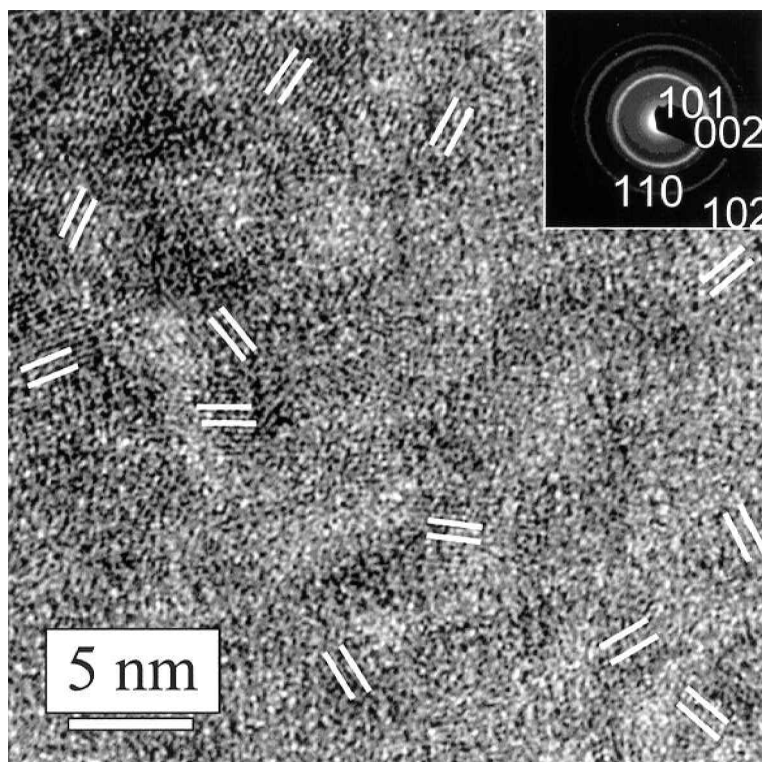

Fig. 3. Microstructure of zircon irradiated at 800°C to a dose of 3 dpa. Randomly oriented ZrO$_2$ nanocrystals are embedded in amorphous SiO$_2$.

We noted previously that this phase decomposition is not inconsistent with the concept of thermal spikes (a transient high-temperature 'spike' occurring during collision cascades) (Meldrum *et al.*, 1998*a*). ZrO_2 has also been reported to occur in naturally occurring metamict zircon (Vance and Anderson, 1972). The present observations suggest that the phase decomposition in natural zircon could be attributed to the effects of ion irradiation damage during periods of elevated temperature. Alternatively, ZrO_2 'colloids' may nucleate in the collision cascades and, over geologic time, gradually grow into discrete particles owing to long-term thermal diffusion effects.

Implications for ABO₄ phosphate and silicate nuclear waste forms

The ion irradiation results in Fig. 2 can be used to predict the crystalline-to-amorphous transformation in monazite- and zircon-based nuclear waste forms. We recently demonstrated that the minimum amount of radioactive material required for amorphization to occur (N_c, in ppm units) is related to the age, t, and temperature, T, of a given mineral grain. N_c can be calculated (Meldrum *et al.*, 1998*b*; Meldrum *et al.*, 1999*b*):

$$N_c(\text{ppm}) = \left[\frac{X}{[1 - e^{C \cdot (1 - T_c/T)}] \cdot (e^{\lambda \cdot t} - 1)} \right] \quad (5)$$

X and C are derived from the ion-irradiation results in Fig. 2 and from the number of α-decay events in the decay chain and the number of atomic displacements per α-decay event (Meldrum *et al.*, 1999*b*). The values of these constants are listed in Table 1 for each of the four compounds investigated here. In Table 1, T_c is the effective critical temperature calculated from equation 4 using $P = 10^{-12}$ dpa/s (equivalent to ~5 wt.% Pu). In equation 5, λ is the decay constant for the radionuclide impurity. The full derivation of equation 5 is lengthy and the reader is referred to the above-mentioned references for a step-by-step procedure.

The value obtained for N_c is of fundamental importance. At a given temperature, grains of a given age with a present-day radionuclide concentration above N_c should be amorphous. If, in fact, they are not amorphous, then equation 5 can be used to calculate the minimum temperature required by the specimen in order to have retained their crystallinity.

An estimate of the accuracy of equation 5 can be obtained by an analysis of crystalline and metamict natural zircon specimens of known age and uranium concentration. In Fig. 4, we plot the literature data for crystalline and metamict zircon spanning a wide range of age and uranium concentrations, as modified from Meldrum *et al.* (1999*b*). The dates of the metamict samples were obtained by dating cogenetic crystalline zircon specimens. As expected, the metamict samples contain a higher concentration of uranium than do the crystalline ones.

Also plotted in Fig. 4 are the values for the present-day critical radionuclide concentration calculated from equation 5, assuming a constant temperature of 100°C (solid lines in Fig. 4). Thus, zircon grains which plot above the upper line should be completely metamict. The upper boundary represents complete amorphization based on electron diffraction in the TEM. In reality, the buildup of radiation damage is a continuous process, so a transition zone between fully crystalline and metamict (as measured by electron diffraction) is also shown. Zircon plotting in this transition zone should be partially amorphous. The 'width' of this transition zone was estimated by assuming that the minimum detectable amorphous fraction, f_a, in the TEM is 35 vol.%, as compared to 95% for 'complete' amorphization (Miller and Ewing, 1992). Assuming direct impact amorphization, the amorphous fraction is related to the dose D_c (Weber, 1990):

$$f_a = 1 - \exp(-BD_c) \quad (6)$$

where B is a constant. Using the above values for f_a in equation 6, the minimum dose observable in the TEM corresponds to 15% of the dose required for amorphization (again judged by electron diffraction). This range is represented in the transition zone plotted in Fig. 4. In general, the model results in Fig. 4 agree rather well with the available data for metamict zircon – especially considering the number of possible variables in the natural specimens (e.g. fluids, temperature, impurities, etc.). The good agreement between the model and the available data suggests that the model is reasonably accurate.

On the basis of this analysis, equation 5 can be used to predict when, in the future, the crystalline-to-amorphous transformation of a Pu-doped mineral waste form will occur. For example, if we assume a 5 wt.% waste loading of [239]Pu in zircon, then N_c is fixed at 5 wt.%, or 43,000 ppm
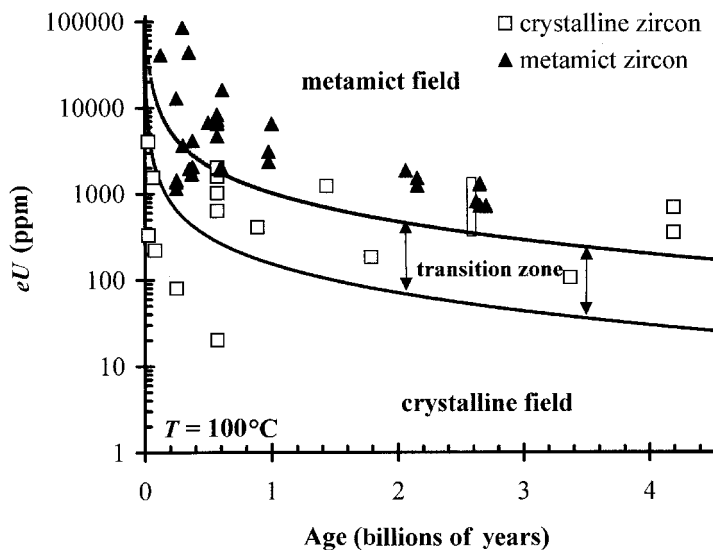
FIG. 4. Calculated critical uranium concentration, N_c, as a function of age in zircon for a temperature of 100°C, modified after Meldrum *et al.* (1999*b*). The solid lines, plotted using equations 4 and 5, demarcate the calculated transition zone between undamaged zircon (lower field) and amorphous zircon (upper field). Literature data for both crystalline (squares) and metamict (triangles) zircon are also plotted (a complete list of references is given in Meldrum *et al.*, 1999*b*). The plotted lines delineate the crystalline-metamict boundary relatively well despite the uncertainty in the thermal history of the various specimens.

Pu. We then need to determine, for any given temperature, how long it will take the material to transform into the amorphous state. In other words, we calculate the relationship between temperature and time for the crystalline-to-amorphous transformation for this fixed value of N_c. Figure 5 shows the results of this calculation for waste loadings of 10, 5, and 1 wt.% ^{239}Pu. The results show that zircon with 10 wt.% Pu would have to be maintained at temperatures in excess of 300°C in order for it to avoid becoming completely amorphous. This value is lowered only slightly by lowering the amount of ^{239}Pu. These temperatures are slightly lower than in our original estimate (Meldrum *et al.*, 1998*b*) but are still higher than the temperatures predicted in currently proposed repository environments (e.g. Weber *et al.*, 1996).

We note that the use of other models in combination with a judicious choice of activation energies can lower the crystalline-to-amorphous transformations to ~150°C for a waste loading of 10 wt.% ^{239}Pu (e.g. see Weber *et al.*, 1996). However, using lower activation energies does

not fit with the data for natural zircon plotted in Fig. 4. In addition, acceptable modelling of a waste form should assume worst-case behaviour. According to the present model, for temperatures <300°C, the worst-case behaviour for zircon is amorphization. Another potential problem arises from the phase decomposition observed during irradiation of zircon at elevated temperatures. Whether or not the phase decomposition could occur at lower temperatures over geologic time periods is not known. However, ZrO_2 has been reported to occur in natural metamict zircon (Vance and Anderson, 1972). Phase decomposition could result in the undesirable formation of grain boundaries and the redistribution of waste products into the ZrO_2 and SiO_2 phases.

A similar analysis for the orthophosphates implies that monazite-based waste forms would not become amorphous or undergo a phase decomposition. A comparison of the values of N_c for $LaPO_4$ with those plotted for zircon on Fig. 4 could not be accomplished because $LaPO_4$ does not become amorphous at 100°C − even at the accelerated dose rates in the laboratory
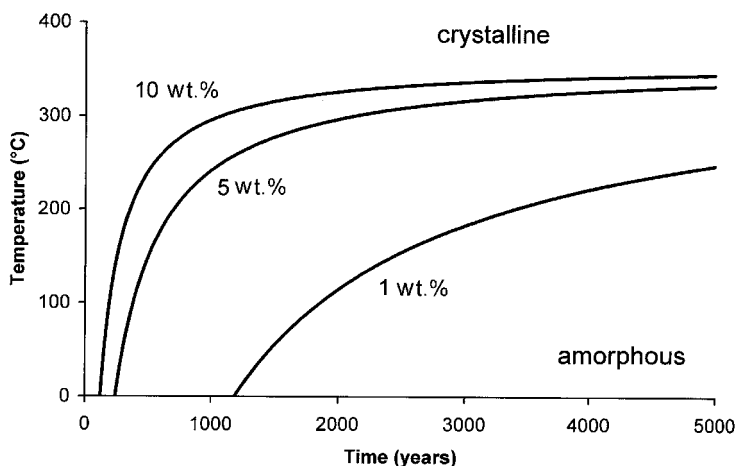
FIG. 5. Calculated time-temperature dependence of the crystalline-to-amorphous transformation in zircon doped with various concentrations of [239]Pu. For simplicity a transition zone is not shown; instead, we show only the upper boundary for complete amorphization, as measured by electron diffraction.

experiments. Although the material is relatively easy to damage by heavy ion irradiation at low temperatures, the annealing kinetics (both thermal and irradiation enhanced) in the orthophosphates are predicted to be sufficiently rapid to prevent amorphization over geologic time periods, even at low temperatures. Additionally, the effects of highly ionizing irradiation (e.g. alpha or beta particles) apparently stabilize the crystalline monazite; in fact, this type of irradiation can lead to complete recrystallization of ion-beam-amorphized $LaPO_4$ and $ScPO_4$ (Meldrum *et al.*, 1997*a*). One potential caveat in the case of monazite is the effect that the impurities may have on the recrystallization kinetics. For example, Meldrum *et al.* (1997*b*) showed that a high concentration of impurities could increase the critical temperature, and in another work, we demonstrated that 1.4 billion-year-old monazite with 17 wt.% ThO_2 (a high concentration of SiO_2 and CaO was also detected) could indeed become metamict (Meldrum *et al.*, 1998*b*).

On the basis of the experimental results presented here, a zircon waste form is expected to undergo irradiation-induced amorphization due to the accumulation of alpha-decay events. Phase decomposition into the component oxides could also occur at higher temperatures. However, at this point too little is known about the kinetics of this process to derive any conclusions for a zircon-based waste form. Note, however, that the leach

rates for amorphous zircon are still orders of magnitude lower than those obtained for borosilicate glass compositions (Ewing, 1982; Helean *et al.*, 1999). In contrast to the case for zircon, monazite is predicted to remain crystalline even for very high waste loadings. Finally, we note that the technique presented here for predicting the crystalline-to-amorphous transformation as a function of actinide content can, in principle, be used for any crystalline waste form for which the kinetics of thermal annealing and amorphization-recrystallization data such as that shown in Fig. 2 are available.

Conclusions

$ZrSiO_4$, monoclinic $ThSiO_4$, $LaPO_4$ and $ScPO_4$ were irradiated by 800 keV Kr^+ ions. The critical temperature, above which amorphization was not induced, was ~400° higher for the silicates than for their phosphate analogues. Materials with the zircon structure (i.e. $ZrSiO_4$ and $ScPO_4$) could be amorphized at slightly higher temperatures (under equivalent irradiation conditions) than the monazite-structure compounds. Above 600°C, $ZrSiO_4$ decomposed to its component oxides as a result of the irradiation. These results were discussed in light of the proposed use of the ABO_4 phosphates and silicates as high-level nuclear waste forms. We applied a recently developed model to predict the crystalline-to-amorphous transformation for these materials as a function of temperature. On

the basis of these calculations, a zircon waste form may become amorphous at temperatures below 300°C or, potentially, may undergo a phase decomposition; whereas, monazite is predicted to remain crystalline.

Acknowledgements

References

Boatner, L.A. (1978) *Letter to the US Department of Energy, Office of Basic Energy Sciences, Division of Materials Science on 28 April detailing the possible uses of monazite as an alternative to borosilicate glass.*

Boatner, L.A. and Sales, B.C. (1988) Monazite. Pp. 495–564 in: *Radioactive Waste Forms for the Future* (W. Lutze and R.C. Ewing, editors). Elsevier, Amsterdam.

Boatner, L.A., Beall, G.W., Abraham, M.M., Finch, C.B., Huray, P.G. and Rappaz, M. (1980) Monazite and other lanthanide orthophosphates as alternate actinide waste forms. Pp. 289–96 in: *Scientific Basis for Nuclear Waste Management*, **2**. (C.J. Northrup, editor). Plenum Press, New York.

Boatner, L.A., Abraham, M.M. and Rappaz, M. (1981) The characterization of nuclear waste forms by EPR spectroscopy. Pp. 181–8 in: *Scientific Basis for Nuclear Waste Management*, **3** (J.G. Moore, editor). Plenum Press, New York.

Burakov, B.E., Anderson, E.B., Rovsha, V.S., Ushakov, S.V., Ewing, R.C., Lutze, W. and Weber, W.J. (1996) Synthesis of zircon for immobilization of actinides. Pp. 33–40 in: *Scientific Basis for Nuclear Waste Management XIX* (W.M. Murphy and D.A. Knecht, editors). Materials Research Society, Pittsburgh, PA.

Ewing, R.C., Haaker, R.F. and Lutze, W. (1982) Leachability of zircon as a function of alpha dose. *Mater. Res. Soc. Symp. Proc.*, **11**, 389–96.

Ewing, R.C., Lutze, W. and Weber, W.J. (1995) Zircon: a host phase for the disposal of weapons plutonium. *J. Mater. Res.*, **10**, 243–6.

Ewing, R.C., Weber, W.J. and Lutze, W. (1996) Waste forms for the disposal of weapons plutonium. Pp. 65–83 in: *Disposal of Ex-Weapons Plutonium as Waste* (E.R. Merz and C.E. Walter, editors). NATO ASI Series, Kluwer Academic Publishers, Dordrecht, The Netherlands.

Gramaccioli, C.M. and Segalstad, T.V. (1978) A uranium- and thorium-rich monazite from a south-alpine pegmatite at Piona, Italy. *Amer. Mineral.,* **63**, 757–61.

Hazen, R.M. and Finger, L.W. (1979) Crystal structure and compressibility of zircon at high pressure. *Amer. Mineral.,* **64**, 196–201.

Helean, K., Lutze, W. and Ewing, R.C. (1999) The dissolution rate of chemically durable materials: zircon. Pp. 297–304 in: *Environmental Issues and Waste Management Technologies IV* (J.C. Marra and G.T. Chandler, editors). American Ceramic Society, Westerville, OH.

McCarthy, G.J., Pepin, J.G. and Davis. D.D. (1980) Crystal chemistry and phase relations in the synthetic minerals of ceramic ware forms: I. Fluorite and monazite structures. Pp. 297–306 in: *Scientific Basis for Nuclear Waste Management*, **2** (C.J. Northrup, editor). Plenum Press, New York.

Meldrum, A., Boatner, L.A. and Ewing, R.C. (1997*a*) Electron irradiation-induced nucleation and growth in amorphous orthophosphates and zircon. *J. Mater. Res.*, **12**, 1816–27.

Meldrum, A., Boatner, L.A., Wang, L.M. and Ewing R.C. (1997*b*) Displacive irradiation effects in the monazite- and zircon-structure orthophosphates (La-LuPO$_4$). *Phys. Rev.*, **B56**, 13805–14.

Meldrum, A., Zinkle, S.J., Boatner, L.A. and Ewing, R.C. (1998*a*) A transient liquid-like state in the displacement cascades of zircon, hafnon and thorite. *Nature*, **395**, 56–8.

Meldrum, A., Boatner, L.A., Weber, W.J. and Ewing, R.C. (1998*b*) Radiation damage in zircon and monazite. *Geochim. Cosmochim. Acta*, **62**, 2509–20.

Meldrum, A., Zinkle, S.J., Boatner, L.A. and Ewing, R.C. (1999*a*) Amorphization, recrystallization and phase decomposition in the ABO$_4$ orthosilicates. *Phys. Rev. B*, **59**, 3981–92.

Meldrum, A., Boatner, L.A., Zinkle, S.J., Wang, S.X., Wang, L.M. and Ewing, R.C. (1999*b*) Effects of dose rate and temperature on the crystalline-to-metamict transformation in the ABO$_4$ orthosilicates. *Canad. Mineral.*, **37**, 207–22.

Miller, M.L. and Ewing, R.C. (1992) Image simulation of partially amorphous materials. *Ultramicroscopy*, **48**, 203–37.

Milligan, W.O., Mullica, D.F., Beall, G.W. and Boatner, L.A. (1982) Structural investigations of YPO$_4$, ScPO$_4$, and LuPO$_4$. *Inorg. Chim. Acta*, **60**, 39–43.

Milligan, W.O., Mullica, D.F., Beall, G.W. and Boatner, L.A. (1983) Structures of ErPO$_4$, TmPO$_4$ and

YbPO$_4$. *Acta Crystallogr.*, **C39**, 23 – 34.

Mullica, D.F., Milligan, W.O., Grossie, D.A., Beall, G.W. and Boatner, L.A. (1984) Ninefold coordination in LaPO$_4$: Pentagonal interpenetrating tetrahedral polyhedron. *Inorg. Chim. Acta*, **95**, 231 – 6.

Mullica, D.F., Grossie, D.A. and Boatner, L.A. (1985) Structural refinements of praseodymium and neodymium orthophosphate. *J. Sol. State Chem.*, **58**, 71 – 7.

Reynolds, R.W., Boatner, L.A., Finch, C.B., Châtelain, A. and Abraham, M.M. (1972) EPR investigations of Er^{3+}, Yb^{2+} and Gd^{3+} in zircon-structure silicates. *J. Chem. Phys.*, **56**, 5607 – 25.

Robinson, M.T. (1983) Computer simulation of collision cascades in monazite. *Phys. Rev. B*, **27**, 5347 – 59.

Speer, J.A. (1982) Zircon. Pp. 67 – 112 in: *Orthosilicates* (P.H. Ribbe, editor). Reviews in Mineralogy, **5**. Mineralogical Society of America, Washington D.C.

Taylor, M. and Ewing, R.C. (1978) The crystal structure of the ThSiO$_4$ polymorphs: huttonite and thorite. *Acta Crystallogr.*, **B34**, 1074 – 9.

Tole, M.P. (1985) The kinetics of dissolution of zircon. *Geochim. Cosmochim. Acta*, **49**, 453 – 8.

Wang, L.M. (1998) Application of advanced electron microscopy techniques to the studies of radiation effects in ceramic materials. *Nucl. Instr. Meth. Phys. Res*., **B141**, 312 – 25.

Vance E.R. and Anderson B.W. (1972) Study of metamict Ceylon zircons. *Mineral. Mag.,* **38**, 605.

Virk, H.S. (1995) Single activation energy model of radiation damage in solid state nucelar track detectors. *Radiation Effects and Defects in Solids*, **133**, 87 – 95.

Weber, W.J. (1990) Radiation-induced defects and amorphization in zircon. *J. Mater. Res.*, **5**, 2687 – 97.

Weber, W.J. (2000) Models and mechanisms of irradiation – induced amorphization in ceramics. *Nucl. Instr. Meth. Phys Rev.* (in press).

Weber, W.J., Ewing, R.C. and Wang, L.M. (1994) The radiation-induced crystalline-to-amorphous transition in zircon. *J. Mater. Res.*, **9**, 688 – 98.

Weber, W.J., Ewing, R.C. and Lutze, W. (1996) Performance assessment of zircon as a waste form for excess weapons plutonium under deep borehole burial conditions. *Mater. Res. Soc. Symp. Proc.*, **412**, 25 – 32.

Weber, W.J., Ewing, R.C., Catlow, C.R.A., Diaz de la Rubia, T., Hobbs, L.W., Kinoshita, C., Matzke, Hj., Motta, A.T., Nastasi, M.A., Salje, E.H.K., Vance, E.R. and Zinkle, S.J. (1998) Radiation effects in crystalline ceramics for the immobilization of high-level nuclear waste and plutonium. *J. Mater. Res.*, **13**, 1434 – 84.

Zinkle, S.J. and Kinoshita, C. (1997) Defect production in ceramics. *J. Nucl. Mater*., **251** 200 – 17.